

## Effect of $B_{12}N_{12}$ junction on the energetic and chemical features of PATO: A density functional theory investigation

Maryam Godarzi<sup>1</sup>, Roya Ahmadi<sup>1\*</sup>, Reza Ghiasi<sup>2</sup>, Mohammad Yousefi<sup>1</sup>

<sup>1</sup>Department of Chemistry, Yadegar-e-Imam Khomeini (RAH) Shahre Rey Branch, Islamic Azad University, Tehran, Iran

<sup>2</sup>Department of Chemistry, Basic Science Faculty, East Tehran Branch, Qiam Dasht, Islamic Azad University, Tehran, Iran

Received 20 March 2018;

revised 30 June 2018;

accepted 16 July 2018;

available online 02 August 2018

### Abstract

In this study, the reaction of 3-Picrylamino-1, 2, 4-Triazole (PATO) with  $B_{12}N_{12}$  was investigated by density functional theory in the B3LYP/6-31G(d) level of theory. There were two possible isomers for reaction of PATO with  $B_{12}N_{12}$  via carbon and nitrogen atoms of triazole ring to the Born atom of  $B_{12}N_{12}$  (I and II-isomers). Thermodynamic parameters of these reactions including formation Enthalpy changes ( $\Delta H_f$ ), Gibbs free energy alterations ( $\Delta G_f$ ) and Heat capacity ( $C_p$ ) were calculated in the temperature range of 300-400K. Variations of density and dipole moment values of PATO after interaction were studied. Also, the frontier orbital energies, HOMO-LUMO gap, chemical hardness ( $\eta$ ), electrophilicity index ( $\omega$ ), charge transferred ( $\Delta N_{max}$ ) and chemical potential ( $\mu$ ) were computed.

**Keywords:**  $B_{12}N_{12}$ ; Density functional theory (DFT); Energetic materials; Thermodynamic parameters; 3-Picrylamino-1, 2, 4-Triazole (PATO).

### How to cite this article

Godarzi M, Ahmadi R, Ghiasi R, Yousefi M. Effect of  $B_{12}N_{12}$  junction on the energetic and chemical features of PATO: A density functional theory investigation. *Int. J. Nano Dimens.*, 2019; 10 (1): 62-68.

## INTRODUCTION

3-Picrylamino-1, 2, 4-Triazole (PATO) has been widely used for blasting and destroying in the wars, owing to its relatively high density. Synthesis and characterization of PATO have been reported in literatures [1-3]. The explosion phenomenon occurs because of the PATO's molecular structure decomposition and its oxidation reaction with the oxygen of the atmosphere [4-6]. PATO is a solid nitroaromatic compound that is synthesized by implementing nitration process on the toluene. This molecule is a toxic yellow solid with high formation heat, due to the existence of many N-N and C-N bonds in its chemical structure [7-10]. One of the most useful properties of PATO is that it can be melted and mixed with other high energy density materials safely [11-13]. Due to the fact that PATO mixtures with oxygen-wealthy compounds can release more energy in comparison to pure PATO, in the 20th century, often a mixture of PATO with

ammonium nitrate was used in the construction of military explosives [14-15]. Generally, the heat released from PATO is considered as a reference for evaluating other explosives because the heat of PATO burning is generated by the reaction between carbons and the atmospheric oxygen. PATO can be considered as a green and environmental friendly material because, after its combustion excessive  $N_2$  gas will be produced in the atmosphere instead of harmful and pollutant gases which are common products of other explosives' combustion [16-19]. Adsorption energy of explosive molecules like 1, 3, 5-Trinitro perhydro-1, 3, 5-triazine (RDX), Octahydro-1, 3, 5, 7-tetranitro-1, 3, 5, 7-tetrazocine (HMX), and so on, with graphene and boron nitride (BN) sheet have been studied by density functional theory methods. These theoretical studies demonstrated that the BN sheet binding with molecules is firmer than graphene ones [20-22]. Also, the incitement of energetic materials

\* Corresponding Author Email: [roya\\_ahmadi\\_chem@yahoo.com](mailto:roya_ahmadi_chem@yahoo.com)

has been investigated by time-dependent density functional theory (TD-DFT) [23-27].

The aim of this study was to evaluate the effect of the nanostructure of  $B_{12}N_{12}$  on energetic properties of PATO by density functional theory (DFT) method.

## COMPUTATIONAL METHODS

Geometrical optimizations and thermodynamic parameters calculations were done by Spartan 10 software [28]. The calculations of systems contain C, O, and N atoms described by the standard 6-31G(d) basis set [29]. Geometry optimization was performed utilizing with the Becke, three-parameter, Lee-Yang-Parr method (B3LYP) [30].

## RESULTS AND DISCUSSIONS

### Energetic aspects

Fig. 1(a, b, c) presents the structures of PATO,  $B_{12}N_{12}$ , and the products of the reaction between these molecules (I-isomer and II-isomer). Absolute

energy values of these molecules are gathered in Table 1. As it can be seen, I-isomer is more stable than II-isomer.

### Dipole moment

The dipole moment values of PATO and  $B_{12}N_{12}$  ... PATO isomers are listed in Table 1. It can be found, the dipole moment values are increased in  $B_{12}N_{12}$  ... PATO isomers in compared to PATO. Dipole moment has a direct relationship with solubility in water and a substance with higher dipole moment is more soluble in polar solvents. Hence, it can be deduced that the solubility of I-isomer and II-isomer is better than pure PATO. In more details, it is obvious that the dipole moment of II-isomer is larger than I-isomer. So, II-isomer has a stronger solubility in comparison to the other one.

### Density of molecules

Density values of the studied molecules are gathered in Table 1. As it is clear, there is not a

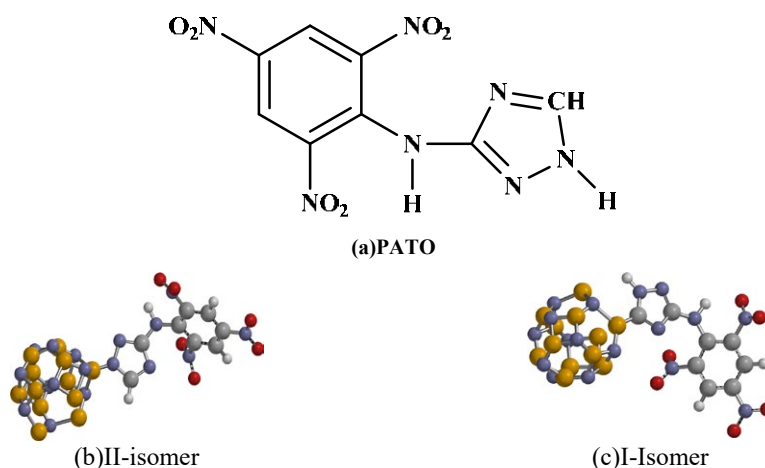


Fig. 1. the structures of optimized molecules (a) PATO, their isomers with  $B_{12}N_{12}$ , (b) II-isomer and (c) I-isomer. Notice: in I-isomer B from  $B_{12}N_{12}$  linked to C from PATO and in II-isomer B from  $B_{12}N_{12}$  linked to N from PATO.

Table 1. Some chemical properties at the B<sub>3</sub>LYP/6-31G level of theory for PATO and its derivatives with  $B_{12}N_{12}$ .

Chemical properties	PATO	I-isomer	II-isomer
Absolute energy (au)	-1120.93	-2004.26	-2003.97
Dipole Moment (debye)	4.09	4.67	15.16
Weight(amu)	295.17	577.97	577.97
Volume( Å <sup>3</sup> )	228.76	452.05	456.94
Area ( Å <sup>2</sup> )	257.24	425.33	436.02
Density=m/v (amu/Å <sup>3</sup> )	1.29	1.28	1.26
E <sub>HOMO</sub> (eV)	-7.31	-5.97	-6.23
E <sub>LUMO</sub> (eV)	3.16	-0.02	-1.04
HLG(eV)	10.47	5.95	5.19
Chemical Hardness (eV)	5.235	2.975	2.595
Chemical Potential (eV)	-2.075	-2.995	-3.635
ω ( eV )	0.4112	1.5076	2.5459
ΔN <sub>max</sub> ( eV )	0.3964	1.0067	1.4008

considerable discrepancy between the density of the pure explosive and its derived products with  $B_{12}N_{12}$ . On the other hand, there are no significant changes in similar bindings of explosive properties such as the bonds between oxygen and nitrogen in nitrite groups and carbon-bonded bonds of benzene ring and nitrite groups of the compounds studied (Table 2 and Fig. 2 (a, b)). Hence, it could be expected that I and II isomers exhibit similar explosive properties to the pure PATO.

#### Electronic structure and thermal stability

The energy gap between the frontier orbitals (highest occupied molecular orbital (HOMO) and lowest unoccupied molecular orbital (LUMO)) are significant properties in numerous chemical processes. The energy values of the HOMO ( $E_{HOMO}$ ) and LUMO ( $E_{LUMO}$ ) reveals the electron donating and electron accepting characters of a molecule, respectively. It has been explored in numerous investigations that the HOMO-LUMO gap may be a significant stability index of the molecules. Exploring of the frontier orbitals is useful to illustration whether the reaction is possible or not and the relative thermal stability of an individual molecule in the gas phase. High HOMO–LUMO gap directly related to the high stability of compounds so these compounds are less reactive in chemical reactions. The energy gap, chemical hardness, chemical potential, electrophilicity and maximum transmitted charge to the system were calculated by the subsequent equations:

$$\text{HOMO-LUMO gap} = E_{LUMO} - E_{HOMO}$$

$$\eta = (E_{LUMO} - E_{HOMO})/2$$

$$\mu \approx (E_{HOMO} + E_{LUMO})/2$$

$$\omega = \mu^2/2\eta$$

$$\Delta N_{max} = -\mu/\eta$$

Table 1, lists these calculated parameters for the PATO and its derivatives with  $B_{12}N_{12}$ .

It can be found, the HOMO and LUMO energy levels increase, and the HOMO–LUMO gap decreases in PATO derivatives with  $B_{12}N_{12}$  in compared to the single PATO. Therefore, it can be concluded that the stability of I and II- isomers are less than PATO molecule. Moreover, energy gap has a direct relationship with the electronic conductivity. Indeed, the materials with lower

HOMO–LUMO gap show better conductance than the substances with higher HOMO–LUMO gap values and in this research, the electronic conductivity of I-Isomer and II-isomer is lower than pure PATO. Thus pure PATO is less conductive than its derivatives with  $B_{12}N_{12}$ .

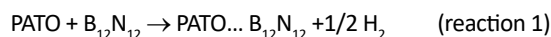
Chemical hardness is the next investigated variable which can estimate the softness of a molecule. In other words, a hard molecule has a large HOMO-LUMO gap and a soft molecule has a small HOMO-LUMO gap. As it is obvious from the table, the chemical hardness of PATO has decreased remarkably from 5.235 (eV) to 2.975 and 2.595 in I and II isomers, respectively. So, after binding with  $B_{12}N_{12}$  the structure of PATO has become more chemically smoother.

Electrophilicity index and maximum amount of electronic charge index were also investigated. The electrophilicity index is a measure of the electrophilic power of a compound when two molecules react with each other. One of them acts as a nucleophile, while the other one behaves as an electrophone system. A compound with higher electrophilicity index demonstrates more electrophilicity.

The most accepted electron charge can be calculated from  $\Delta N_{max}$  parameter. The maximum amount of electronic charge index ( $\Delta N_{max}$ ) is the most electron charge which a system can accept. A positive  $\Delta N_{max}$  indicates that charge flows to the system or in other words, the system acts as an electron acceptor. But a negative  $\Delta N_{max}$  value indicates that the system likes to donate its electrons and acts as a lewis base. As it can be observed from the table, the electrophilicity and  $\Delta N_{max}$  of PATO has enhanced significantly after its attachment to the studied nanostructure. In other words, its affinity for accepting electron has defused dramatically.

#### Thermodynamic parameters

Owing to the fact that, the purpose of this study is to find out the effects of  $B_{12}N_{12}$  on the chemical and energetic properties of PATO, It seems logical to investigate the feasibility of the reaction between the explosive substance and  $B_{12}N_{12}$ . In this regards, thermodynamic parameters of the reaction between PATO and  $B_{12}N_{12}$  ( $\Delta H_r$ ,  $\Delta G_r$ ,  $K_{th}$  and  $C_v$ ) were calculated and checked out on the basis of the following reaction:



These parameters are evaluated by the following equations (X=H and G):

$$\Delta X_f (T K) = \sum (\epsilon_{0+} X_{corr})_{Products} - \sum (\epsilon_{0+} X_{corr})_{Reactants} \quad (1)$$

enthalpies or free energy ( $X_{corr}$ ) =  $\epsilon_{0+} X$

$$\Delta X_f = \Delta X_{formation} \quad (2)$$

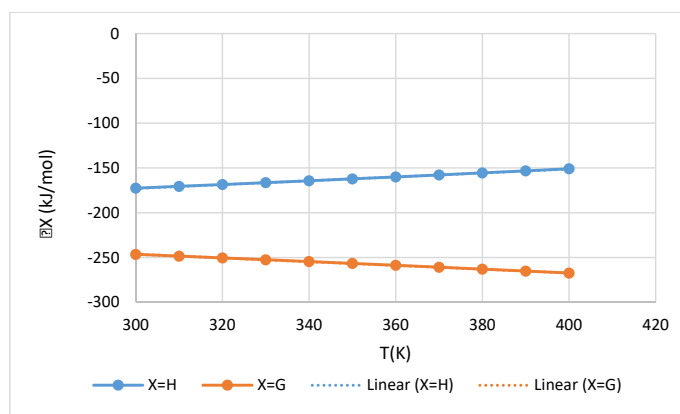
$$\Delta X_f (T K) = \sum (X)_{Products} - \sum (X)_{Reactants}$$

Sum of the electronic energy ( $\epsilon_0$ ) and thermal

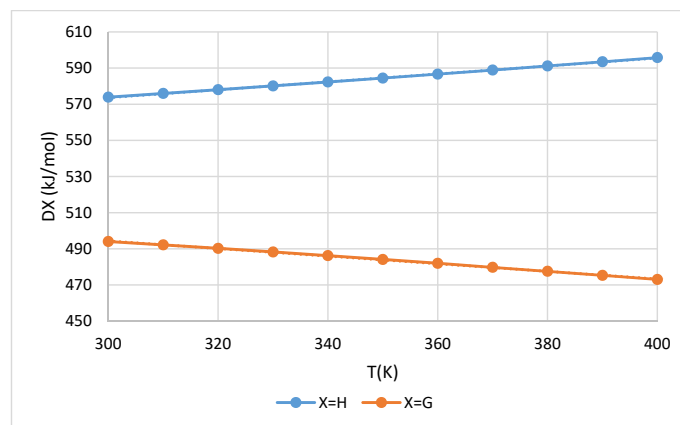
According to the equations 1-2 can be written:

Table 2. The Results of Enthalpy and Gibbs Free Energy and thermodynamic equilibrium constant (Kth) in the range of 300-400 K at the level B<sub>3</sub>lyp / 6-31G(d) for derivative material of PATO with B<sub>12</sub>N<sub>12</sub>.

T(K)	$\Delta H_f$ (kJ/mol)		$\Delta G_f$ (kJ/mol)		$K_{th}$	
	II-isomer	I-isomer	II-isomer	I-isomer	II-isomer	I-isomer
300	573.8813007	-172.6177744	494.0100007	-246.4890744	2.80787E-87	1.53257E+43
310	575.9317007	-170.6028744	492.1505007	-248.4387744	5.94518E-87	3.36521E+43
320	578.0098007	-168.5595744	490.2273007	-250.4635744	1.29156E-86	7.6166E+43
330	580.1237007	-166.4816744	488.2483007	-252.5015744	2.86972E-86	1.7331E+44
340	582.2695007	-164.3813744	486.2102007	-254.5400744	6.53008E-86	3.94433E+44
350	584.4490007	-162.2453744	484.1042007	-256.6024744	1.52719E-85	9.06379E+44
360	586.6628007	-160.0603744	481.9528007	-258.7289744	3.63768E-85	2.13736E+45
370	588.8881007	-157.8424744	479.7280007	-260.8810744	8.92512E-85	5.09249E+45
380	591.1591007	-155.5756744	477.5320007	-263.0360744	2.1645E-84	1.21476E+46
390	593.4754007	-153.2897744	475.2947007	-265.1912744	5.3375E-84	2.89792E+46
400	595.8079007	-150.9583744	473.0559007	-267.3718744	1.31698E-83	6.98445E+46



(a) I-Isomer



b) II-Isomer

Fig. 2(a, b). Dependency of  $\Delta H$  and  $\Delta G$  on the temperature for the synthesis reaction of nano derivatives material of PATO with B<sub>12</sub>N<sub>12</sub> at different temperatures.

$$\Delta H_f = [X_{\text{PATO... B}_{12}\text{N}_{12}} + 1/2X_{\text{H}_2}] - [X_{\text{PATO}} + X_{\text{B}_{12}\text{N}_{12}}] \quad (3)$$

The thermodynamic equilibrium constant of the desired procedure was also calculated from the succeeding equation:

$$K = \exp (- \Delta G_f / RT) \quad (4)$$

Thermodynamic parameters of the reaction are listed in Table 2. As it can be witnessed,  $\Delta H_f$  values are negative and positive for I-isomer and II-isomer, respectively. Therefore, it can be deduced that  $\text{B}_{12}\text{N}_{12}$  reaction with the carbon atom of PATO is exothermic while the  $\text{B}_{12}\text{N}_{12}$  reaction with the nitrogen atom of PATO is endothermic. The effect of temperature variation on  $\Delta H_f$  values was also inspected in the temperature range of 300-400 K. As it is obvious from the table, by increasing the temperature  $\Delta H_f$  values of the II-isomer have also risen. But by contrast, the  $\Delta H_f$  values of the I-isomer have reduced proportionally by incrementing of temperature. This phenomenon reveals that the formation process of the I-isomer has become more exothermic by temperature increasing whereas the formation procedure of the II-isomer has become more endothermic by temperature incrementing. In fact,  $\text{B}_{12}\text{N}_{12}$  reacts with PATO through the carbon atom (Fig. 2). There are good linear relationships between  $\Delta H$  and temperature:

$$\text{I-isomer: } \Delta H = 0.2165 T - 237.82; \quad R^2 = 0.9995$$

$$\text{II-isomer: } \Delta H = 0.2193 T + 507.87; \quad R^2 = 0.9996$$

Gibbs free energy changes ( $\Delta G_f$ ) and

thermodynamic equilibrium constant ( $K_{th}$ ) of the desired reactions are calculated and listed in Table 2. It can be found,  $\Delta G_f$  and  $K_{th}$  values for the formation reaction of the I-isomer are considerably negative. Therefore, it can be predicted this process is spontaneous. It should be noted that the temperature has a substantial influence on the formation reaction of I-isomer because the acquired results show that by enhancing the temperature the values of  $\Delta G_f$  and  $K_{th}$  have become more negative and positive respectively. Hence, temperature rising can catalyze this reaction. However, it seems the formation reaction of the II-isomer is non-spontaneous due to the achieved positive  $\Delta G_f$  and small  $K_{th}$  values (Fig. 2 (a, b)). It can be observed good linear relationships between  $\Delta G$  and temperature:

$$\text{I-isomer: } \Delta G = -0.2092 T - 183.54; \quad R^2 = 0.9997$$

$$\text{II-isomer: } \Delta G = -0.2105 T + 557.55; \quad R^2 = 0.9991$$

The calculated Specific heat capacity ( $C_v$ ) Values for the derivative products of PATO and  $\text{B}_{12}\text{N}_{12}$  at different temperatures are presented in Table 2 and (Fig. 3). The obtained heat capacity values indicate that the heat capacity of PATO is lower than its derivatives with  $\text{B}_{12}\text{N}_{12}$  in both of the I-isomer and II-isomer at all of evaluated temperatures. The specific heat capacity is the amount of heat per unit mass required to raise the temperature by one degree Celsius, so it causes low energy increases the material temperature. Less specific heat capacity values of PATO shows that energetic properties of PATO are greater than

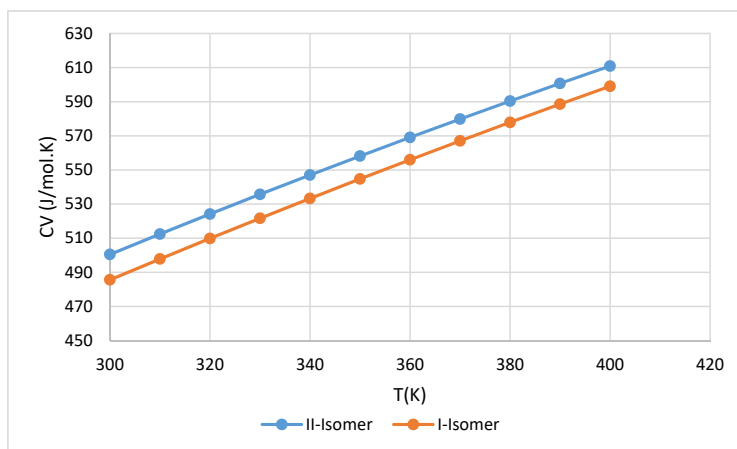


Fig. 3. Chart of heat capacity ( $C_v$ (J/mol.K)) in the range of 300-400 K at the level  $\text{B}_3\text{LYP} / 6\text{-}31\text{G}$  for derivative material of PATO with  $\text{B}_{12}\text{N}_{12}$ .

Table 3. The results of specific heat capacity (Cv(J/mol.K)) in the temperature range of 300-400 K at the level B<sub>3</sub>LYP / 6-31G(d) for derivative material of PATO with B<sub>12</sub>N<sub>12</sub> reaction.

Temperature	Cv(J/mol.K)		
	PATO	II-isomer	I-isomer
300	246.8222	500.5042	485.6074
310	253.0734	512.4355	497.8184
320	259.2605	524.1663	509.8365
330	265.3804	535.6970	521.6618
340	271.4300	547.0285	533.2947
350	277.4064	558.1622	544.7359
360	283.3067	569.0993	555.9862
370	289.1284	579.8417	567.0465
380	294.8687	590.3911	577.9175
390	300.5256	600.7492	588.6002
400	306.097	610.9179	599.0956

its derivations. Heat capacity is increased with increasing molecular weight which is illustrated in Table 3 and Fig. 3. Therefore, the sensitivity of PATO to the shock and heat has reduced sharply after junction to B<sub>12</sub>N<sub>12</sub>.

## CONCLUSIONS

Researching on explosive materials is a significant challenge in front of the scholars because it can endanger the safety and health of the scientists. In addition, it needs some expensive and sophisticated instruments which are not affordable in every laboratory. But fortunately, theoretical methods can provide valuable information about this type of substance which is in a good agreement with experimental methods. Moreover, computational techniques are economical and extremely safe especially in this field of science. In this regard, the reaction of PATO with B<sub>12</sub>N<sub>12</sub> was investigated in this research in the temperature range of 300-400 K at two configurations. The obtained  $\Delta H_f$  and  $\Delta G_f$  values were negative for I-isomer. But on the other hand these parameters are positive for II-isomer. Therefore, B<sub>12</sub>N<sub>12</sub> reaction with the carbon atom of PATO is experimentally feasible because it is exothermic and spontaneous. But on the other hand, the B<sub>12</sub>N<sub>12</sub> reaction with the nitrogen atom of PATO is an endothermic and non-spontaneous. The density of pure PATO and its derivatives with B<sub>12</sub>N<sub>12</sub> were very close to each other. Whilst, the specific heat capacity of the I-isomer and II-isomer were considerably greater than single PATO and this phenomenon is evidence which proved that the sensitivity to heat and shock of PATO derivatives with the evaluated nanostructure is lower than single PATO. Therefore, I-isomer and II-isomer have higher safety than PATO. So, PATO derived products with B<sub>12</sub>N<sub>12</sub> has the ability to be used as an potential

explosive in the construction of war weapons.

## CONFLICT OF INTEREST

The authors declare that there is no conflict of interests regarding the publication of this review article.

## REFERENCES

- [1] Ayoub K., Van Hullebusch E. D., Cassir M., Bermond A., (2010), Application of advanced oxidation processes for TNT removal: A review. *J. Hazard Mater.* 178: 10-28.
- [2] Panz K., Miksch K., (2012), Phytoremediation of explosives (TNT, RDX, HMX) by wild-type and transgenic plants. *J. Environ. Manage.* 113: 85-92.
- [3] Zhang J. G., Niu X. Q., Zhang S. W., Zhang T. L., Huang H. S., Zhou Z. N., (2011), Novel potential high-nitrogen-content energetic compound: Theoretical study of diazido-tetrazole (CN10). *Comput. Theor. Chem.* 964: 291-297.
- [4] Wu J. T., Zhang J. G., Yin X., He P., Zhang T. L., (2014), Synthesis and characterization of the nitrophenol energetic ionic salts of 5, 6, 7, 8-tetrahydrotetrazolo [1,5-b] [1,2,4] triazine. *Eur. J. Inorg. Chem.* 27: 4690-4695.
- [5] Zhao Z., Du Z., Han Z., Zhang Y., He C., (2016), Nitrogen-rich energetic salts: Both cations and anions contain tetrazole rings. *J. Energ. Mater.* 34: 183-196.
- [6] Lin Q. H., Li Y. C., Qi C., Liu W., Wang Y., Pang S. P., (2013), Nitrogen-rich salts based on 5-hydrazino-1H-tetrazole: A new family of high-density energetic materials. *J. Mater. Chem. A.* 1: 6776-6785.
- [7] Joo Y. H., Shreeve J. M., (2010), High-density energetic mono- or bis (Oxy)-5-nitroiminotetrazoles. *Angew. Chem. Int. Ed.* 49: 7320-7323.
- [8] Zhang J., Shreeve J. M., (2010), 3, 3'-dinitroamino-4, 4'-azoxyfurazan and its derivatives: An assembly of diverse N-O building blocks for high-performance energetic materials. *J. Am. Chem. Soc.* 136: 4437-4445.
- [9] Talawar M. B., Sivabalan R., Mukundan T., Muthurajan H., Sikder A. K., Gandhe B. R., Subhananda R. A., (2009), Environmentally compatible next generation green energetic materials (GEMs). *J. Hazard. Mater.* 161: 589-607.
- [10] Bahrami Panah N., Vaziri R., (2015), Structure and electronic properties of single-walled zigzag BN and B<sub>3</sub>C<sub>2</sub>N<sub>3</sub> nanotubes using first-principles methods. *Int. J. Nano.*

- Dimens.* 6: 157-165.
- [11] Vovusha H., Sanyal B., (2015), DFT and TD-DFT studies on the electronic and optical properties of explosive molecules adsorbed on boron nitride and graphene nano flakes. *RSC. Adv.* 5: 4599-4608.
- [12] Cooper J. K., Grant C. D., Zhang J. Z., (2013), Experimental and TD-DFT study of optical absorption of six explosive molecules: RDX, HMX, PETN, TNT, TATP, and HMTD. *J. Phys. Chem. A.* 117: 6043-6051.
- [13] Zohari N., Abrishami F., Ebrahimikia M., (2016), Investigation of the effect of various substitutions on the density of tetrazolium nitrate salts as green energetic materials. *Zaac.* 13: 749-760.
- [14] Ahmadi R., Pirahan Foroush M., (2014), Fullerene effect on chemical properties of antihypertensive clonidine in water phase. *Annals of Military & Health Sci. Res.* 12: 39-43.
- [15] Blackmore K. J., Lal N., Ziller J. W., Heyduk A. F., (2008), Catalytic reactivity of a zirconium(IV) redox-active ligand complex with 1, 2-diphenylhydrazine. *J. Am. Chem. Soc.* 130: 2728-2729.
- [16] Ghiasi R., Sadeghi N., (2017), Evolution of the interaction between  $C_{20}$  cage and  $Cr(CO)_5$ : A solvent effect, QTAIM and EDA investigation. *J. Theoret. Comput. Chem.* 16: 1750007-1750010.
- [17] Ghiasi R., Manoochehri M., Lavasani R., (2016), DFT and TD-DFT study of benzene and borazines containing chromophores for DSSC materials. *Russ. J. Inorg. Chem.* 61: 1267-1273.
- [18] Ghiasi R., Amini E., (2015), Theoretical view on structure, chemical reactivity, aromaticity and 14N NQR parameters of iridapyridine isomers. *J. Struct. Chem.* 56: 1458-1467.
- [19] Fashami M. Z., Ghiasi R., (2015), Theoretical study of solvent and substituent effects on the structure, 14N NQR and electronic spectra of  $[Cr(CO)5py]$ . *J. Struct. Chem.* 56: 1474-1482.
- [20] Ghiasi R., Mokarram E. E., (2011), Theoretical investigation on geometries and aromaticity of heterocyclic platinabenzenes. *Russ. J. Coord. Chem.* 37: 463-467.
- [21] Ahmadi R., Mirkamali E. S., (2016), Determination of thermodynamic parameters of produced materials from (ATTz) with boron nitride nano-cages in different conditions of temperature, with DFT method. *J. Phys.Theoret. Chem. I. A.U.* 13: 297-302.
- [22] Shemshaki L., Ahmadi R., Nikmaram F. R., (2017), Study of synthesis of 1-(4-nitrophenyl)-1H-tetrazole from the reaction of (dihydroxyamino) benzonitrile with Sodium azide in different temperature conditions, the DFT method. *Am. J. Oil Chem. Technol.* 5: 1-9.
- [23] Ahmadi R., Madahzadeh Darini N., (2016), Study of 5-Picrylamino-1, 2, 3, 4-tetrazole (PAT) with nanostructures of fullerene and boron nitride nano-cages in different conditions of temperature, using density functional theory. *Int. J. Bio-Inorg. Hybrid Nanomater.* 5: 273-278.
- [24] Ahmadi R., Shemshaki L., (2017), The synthesis of  $\alpha$ , 2, 4, 6-tetranitrotoluene from the reaction of 2, 4, 6-trinitrotoluene (TNT) with Fluorotrinitromethane in different temperature conditions, the DFT method. *Am. J. Oil Chem. Technol.* 5: 6-11.
- [25] Ahmadi R., Boroushaki T., Ezzati M., (2015), The usage comparison of occupancy parameters, gap band energy,  $\Delta N_{max}$  at xylometazoline medicine ratio its medical conveyer nano. *Int. J. Nano Dimens.* 6: 19-22.
- [26] Ahmadi R., Pirahan-Foroush M., (2014), Ab initio studies of fullerene effect on chemical properties of naphazoline drop. *Annals of Military & Health Sci. Res.* 12: 86-90.
- [27] Ahmadi R., Ezzati M., Boroushaki T., (2014), Computational study of chemical properties of Xylometazoline and the connected form to fullerene (C60) as a medicine nano carrier. *Int. J. Bio-Inorg. Hybd. Nanomat.* 3: 23-27.
- [28] Deppmeier B. J., Driessen A. J., Hehre T. S., Hehre W. J., Johnson J. A., Klunzinger P. E., Leonard J. M., Pham I. N., Pietro W. J., Yu J., (2008), "Spartan '10, Version 1.0.0,Wavefunction", Inc., Irvine, CA.
- [29] Hariharan P. C., Pople J. A., (1973), Influence of polarization functions on molecular-orbital hydrogenation energies. *Theoret. Chimica Acta.* 28: 213-222.
- [30] Becke A. D., (1993), Density-functional thermochemistry. III. The role of exact exchange. *J. Chem. Phys.* 98: 5648-5652.